

Traffic of interacting ribosomes: effects of single-machine mechano-chemistry on protein synthesis

Aakash Basu¹ and Debashish Chowdhury^{*1}

¹*Department of Physics, Indian Institute of Technology, Kanpur 208016, India.*

(Dated: March 31, 2022)

Many *ribosomes* simultaneously move on the same messenger RNA (mRNA), each separately synthesizing the protein coded by the mRNA. Earlier models of ribosome traffic represent each ribosome by a “self-propelled particle” and capture the dynamics by an extension of the totally asymmetric simple exclusion process (TASEP). In contrast, here we develop a theoretical model that not only incorporates the *mutual exclusions* of the interacting ribosomes, but also describes explicitly the mechano-chemistry of each of these individual cyclic machines during protein synthesis. Using analytical and numerical techniques of non-equilibrium statistical mechanics, we analyze this model and illustrate its power by making experimentally testable predictions on the rate of protein synthesis in real time and the density profile of the ribosomes on some mRNAs in *E-Coli*.

Translation, the process of synthesis of proteins by decoding genetic information stored in the mRNA, is carried out by *ribosomes*. Understanding the physical principles underlying the mechanism of operation of this complex macromolecular machine [1] will not only provide insight into the regulation and control of protein synthesis, but may also find therapeutic applications as ribosome is the target of many antibiotics [2].

Most often many ribosomes move simultaneously on the same mRNA strand while each synthesises a protein. In all the earlier models of collective traffic-like movements of ribosomes [3, 4, 5, 6, 7, 8, 9], the entire ribosome is modelled as a single “self-propelled particle” ignoring its molecular composition and architecture. Moreover, in these models the inter-ribosome interactions are captured through hard-core mutual exclusion and the dynamics of the system is formulated in terms of rules that are essentially straightforward extensions of the TASEP [10].

In reality, the mechanical movement of each ribosome is coupled to its biochemical cycle. The earlier TASEP-like models cannot account for those aspects of spatio-temporal organization that depend on the detailed mechano-chemical cycle of each ribosome. In this letter we develop a “unified” model that not only incorporates the hard-core mutual exclusion of the interacting ribosomes, but also captures explicitly the essential steps in the biochemical cycle of each ribosome, including GTP (guanine triphosphate) hydrolysis, and couples it to its mechanical movement during protein synthesis. Consequently, in the low-density limit, our model accounts for the protein synthesis by a single isolated ribosome while at higher densities the same model predicts not only the rate of protein synthesis but also the collective density profile of the ribosomes on the mRNA strand.

We represent the mRNA chain, consisting of L codons, by a one-dimensional lattice of length $L + \ell - 1$ where each

of the first L sites from the left represents a single codon (i.e., a triplet of nucleotides). We label the sites of the lattice by the integer i ; the sites $i = 1$ and $i = L$ represent the start codon and the stop codon, respectively.

The smaller sub-unit of the ribosome, which is known to bind with the mRNA, is represented by an *extended particle* of length ℓ (in the units of the size of a codon), as shown in fig.1(a) ($\ell = 12$ for all results reported here). [4, 5, 6, 7, 8, 9], Thus, the smaller subunit of each ribosome covers ℓ codons at a time (see fig.1(a)). According to our convention, the *position* of such a ribosome on the mRNA strand will be given by the position of the lattice site covered by the *left* edge of its smaller subunit. Each ribosome moves forward by only one site in each step as it must translate successive codons one by one. The mutual interactions of the ribosomes translocating on the same mRNA is taken into account by imposing the constraint of mutual exclusion.

The process of translation itself can be divided into three main stages: (a) *initiation*, (b) *elongation*, and (c) *termination*. Since our model is *not* intended to describe initiation and termination in detail, we represent initiation and termination by the two parameters α and β , respectively (see fig.1(a)). If the first ℓ sites on the mRNA are vacant, this group of sites is allowed to be covered by a ribosome, from the pool of unbound ribosomes, with probability α in the time interval Δt (in all our numerical calculations we take $\Delta t = 0.001$ s). Similarly, if the rightmost ℓ sites of the mRNA lattice are covered by a ribosome, i.e., the ribosome is bound to the L -th codon, the ribosome gets detached from the mRNA with probability β in the time interval Δt . Moreover, since α is the probability of attachment in time Δt , the probability of attachment per unit time (which we call ω_α) is the solution of the equation $\alpha = 1 - e^{-\omega_\alpha \times \Delta t}$.

To our knowledge, all the earlier models of ribosome traffic on mRNA [3, 4, 5, 6, 7, 8, 9], describe elongation also by a single parameter, namely, the rate q of hopping of a ribosome from one codon to the next. In contrast, we model the mechano-chemistry of elongation

*Corresponding author: debch@iitk.ac.in

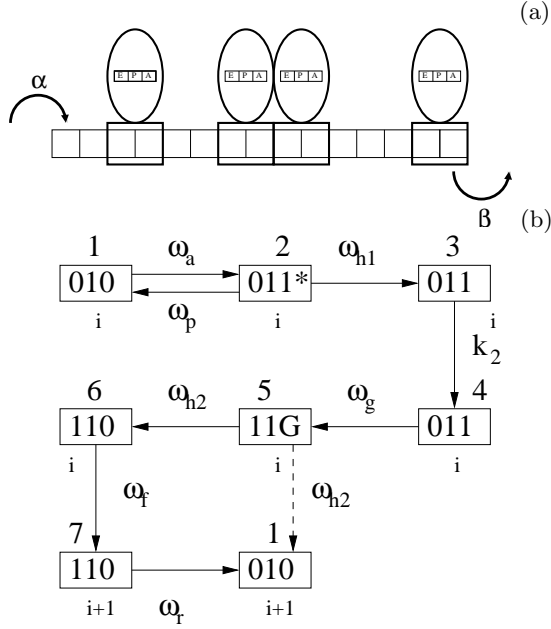


FIG. 1: (a) The mRNA is represented by a one-dimensional lattice each site of which corresponds to a distinct codon; the smaller subunit of the ribosome (represented schematically by the rectangle) can cover simultaneously ℓ codons ($\ell = 2$ in this figure) while the letters E, P, A denote the three binding sites on its larger subunit. The parameters α and β capture the effective rates of initiation and termination of translation. (b) The biochemical cycle of a single ribosome during the elongation stage. Each box represents a distinct state of the ribosome. The index below the box labels the codon on the mRNA with which the smaller subunit of the ribosome binds. The number above the box labels the biochemical state of the ribosome. Within each box, 1(0) represents presence (absence) of tRNA on binding sites E, P, A. 1* is a EF-Tu bound tRNA and G is a EF-G GTPase. The symbols accompanied by the arrows define the rate constants for the corresponding transitions. The dashed arrow represents the approximate pathway we have considered in our model.

in detail (fig.1(b)). In state 1, the ribosome begins with a tRNA bound to the site P. Binding of a fresh tRNA-EF-Tu complex to site A causes the transition $1 \rightarrow 2$. The EF-Tu has a GTP part which is then hydrolyzed to GDP, driving the transition $2 \rightarrow 3$. Next, the phosphate group, a product of the hydrolysis, leaves resulting in the state 4. This hydrolysis, finally, releases the EF-Tu, and the peptide bond formation becomes possible. After this step, the tRNAs shift from site P to E and from site A to P; the site A becomes occupied by EF-G, in the GTP bound form, resulting in the state 5. Hydrolysis of the GTP to GDP and the release of EF-G drives the transition $5 \rightarrow 6$. The transition $6 \rightarrow 7$ is accompanied by conformational changes that are responsible for pulling the mRNA-binding smaller subunit by one step forward. Finally, the tRNA on site A is released, resulting in completion of one biochemical cycle; in the process

the ribosome moves forward by one codon (i.e., one step on the lattice).

However, in setting up the rate equations below, we treat the entire transition $5 \rightarrow 6 \rightarrow 7 \rightarrow 1$ as, effectively, a single step transition from 5 to 1, with rate constant ω_{h2} . Thus, throughout this paper we work with a simplified model where each biochemical cycle during the elongation process consists of *five* distinct states.

The modelling strategy adopted here for incorporating the biochemical cycle of ribosomes is similar to that followed in the recent work [11] on single-headed kinesin motors KIF1A. However, the implementation of the strategy is more difficult here not only because of the higher complexity of composition, architecture and mechanochemical processes of the ribosomal machinery and but also because of the *heterogeneity* of the mRNA track [12].

Let $P_\mu(i)$ be the probability of finding a ribosome at site i , in the chemical state μ . Then, $P(i) = \sum_{\mu=1}^5 P_\mu(i)$, is the probability of finding a ribosome at site i , irrespective of its chemical state. Moreover, if a site is *not* covered by any part of any ribosome, we'll say that the site is occupied by a "hole". Furthermore, by the symbol $Q(i|j)$ we denote the conditional probability that, given a ribosome at site i , there is a hole at the site j . The master equations for the probabilities $P_\mu(i)$ are given by

$$\begin{aligned} \frac{dP_1(i)}{dt} = & \omega_{h2}P_5(i-1)Q(i-1|i-1+\ell) \\ & + \omega_pP_2(i) - \omega_aP_1(i) \end{aligned} \quad (1)$$

$(i \neq 1)$

$$\frac{dP_2(i)}{dt} = \omega_aP_1(i) - (\omega_p + \omega_{h1})P_2(i) \quad (2)$$

$$\frac{dP_3(i)}{dt} = \omega_{h1}P_2(i) - k_2P_3(i) \quad (3)$$

$$\frac{dP_4(i)}{dt} = k_2P_3(i) - \omega_gP_4(i) \quad (4)$$

$$\begin{aligned} \frac{dP_5(i)}{dt} = & \omega_gP_4(i) - \omega_{h2}P_5(i)Q(i|i+\ell) \end{aligned} \quad (5)$$

$(i \neq L)$

However, the equations for $P_1(1)$ and $P_5(L)$ have the special forms

$$\frac{dP_1(1)}{dt} = \omega_a \left(1 - \sum_{s=1}^{\ell} P(s) \right) + \omega_pP_2(1) - \omega_aP_1(1) \quad (6)$$

$$\frac{dP_5(L)}{dt} = \omega_gP_4(L) - \beta P_5(L). \quad (7)$$

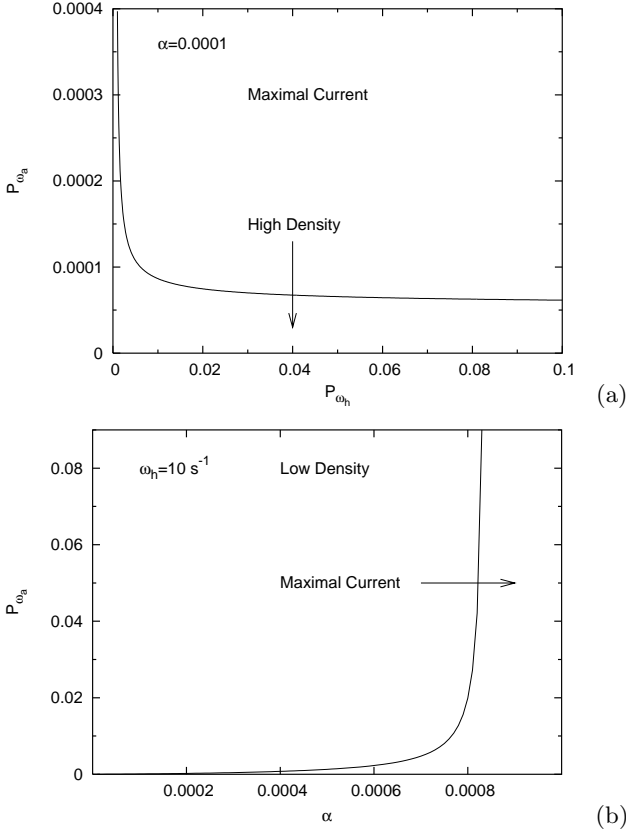


FIG. 2: Phase diagram in (a) $P_{\omega_h} - P_{\omega_a}$ plane and (b) $\alpha - P_{\omega_a}$ plane. $\omega_g = 25 \text{ s}^{-1}$, $\omega_P = 0.0028 \text{ s}^{-1}$, $k_2 = 2.4 \text{ s}^{-1}$, $\beta = 1$.

Because of the finite length of the codon sequence between the start and stop codons, the open boundary conditions (OBC) are more realistic than the periodic boundary conditions (PBC). However, we begin with a calculation of the flux of the ribosomes in the steady-state by imposing PBC as the results for this artificial situation are required for a derivation of the dynamical phase diagram of the system under OBC. Under PBC, $P_\mu(i)$ for all i are governed by the equations (1)-(5). Moreover, under the PBC, only four of the five equations (1)-(5) are independent because $P(i) = \sum_{\mu=1}^5 P_\mu(i) = N/L = \rho$ where ρ , the number density of the ribosomes, is a constant independent of time; therefore, we do not need to consider equation (1) for $P_1(i)$ explicitly. In the steady state, all time derivatives vanish and because of the translational invariance of this state under PBC, the index i can be dropped. It is straightforward to show [13] that, for PBC,

$$Q(i|i+\ell) = \frac{L - N\ell}{L + N - N\ell - 1}. \quad (8)$$

Therefore, under the PBC, equations (2-5) can be solved, using (8), to obtain

$$P_5 = \frac{P}{1 + \frac{\omega_{h2}(L-N\ell)}{L+N-N\ell-1} \left[\frac{1}{k_{eff}} \right]} \quad (9)$$

where

$$\frac{1}{k_{eff}} = \frac{1}{\omega_g} + \frac{1}{k_2} + \frac{1}{\omega_{h1}} + \frac{1}{\omega_a} + \frac{\omega_p}{\omega_a \omega_{h1}} \quad (10)$$

The flux of ribosomes J , under PBC, obtained from $J = \omega_{h2} P_5 Q(i|i+\ell)$, is

$$J = \frac{\omega_{h2} \rho (1 - \rho \ell)}{(1 + \rho - \rho \ell) + \Omega_{h2} (1 - \rho \ell)} \quad (11)$$

where $\Omega_{h2} = \omega_{h2}/k_{eff}$. The rate of protein synthesis by a single ribosome is ℓJ . This mean-field estimate is a reasonably good approximation to the data obtained by direct computer simulations [13].

It can be shown [13] that, for OBC,

$$Q(i|i+\ell) = \frac{1 - \sum_{s=1}^{\ell} P(i+s)}{1 - \sum_{s=1}^{\ell} P(i+s) + P(i+\ell)} \quad (12)$$

and the corresponding flux can be obtained from

$$J = \omega_a \left(1 - \sum_{s=1}^{\ell} P_s \right) \quad (13)$$

Motivated by the recent measurements [14, 15] of the number of bound ribosomes on the mRNA, we have computed the detailed density profiles of the ribosomes and also drawn the phase diagrams in the spirit of the similar plots of non-equilibrium dynamical phases of totally asymmetric simple exclusion process [10].

The probabilities α and β of initiation and termination are incorporated into the model by connecting the ends of the mRNA strand to two hypothetical reservoirs with appropriate densities ρ_- and ρ_+ , respectively [5]. The extremum principle [10, 16] then relates the flux j in the open system to the flux $J(\rho)$ for a closed periodic system with the same dynamics:

$$j = \begin{cases} \max J(\rho) & \text{if } \rho_- > \rho > \rho_+ \\ \min J(\rho) & \text{if } \rho_- < \rho < \rho_+ \end{cases}$$

For systems with a single maximum in the function $J(\rho)$, at $\rho = \rho_*$, such as equation (11), the maximal current phase sets in when $\rho_- > \rho_* > \rho_+$. By differentiating equation (11), we find [13]

$$\rho_* = \frac{-\ell(1 + \Omega_{h2}) + \sqrt{\ell(1 + \Omega_{h2})}}{\ell(1 - \ell - \Omega_{h2}\ell)} \quad (14)$$

It can also be shown that [13]

$$\rho_- = \frac{\alpha(1 - \frac{\ell}{L})(1 + \Omega_{h2})}{P_{\omega_h} - \alpha(1 + \Omega_{h2})(1 - \ell)} \quad (15)$$

where P_{ω_h} is the probability of hydrolysis in the time Δt , and that $\rho_+ = 0$. Similarly, the probability of attachment of a $aa-tRNA$ in time Δt is denoted by P_{ω_a} . Thus, the

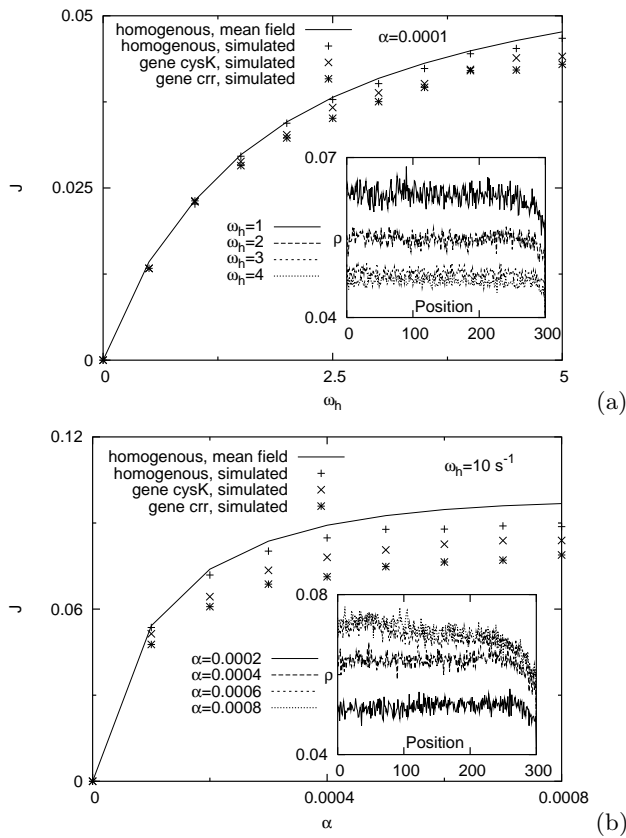


FIG. 3: Flux of ribosomes plotted against (a) ω_h and (b) α for the genes *crr* (170 codons) and *cysK* (324 codons) of *Escherichia coli* K-12 strain MG1655, as well as the corresponding curve for a homogeneous mRNA strand of 300 codons. The insets show the average density profiles on a hypothetical *homogeneous* mRNA track for four different values of (a) ω_h and (b) α , for fixed $\omega_a = 25 \text{ s}^{-1}$.

phase boundaries between the various phases have been

obtained by solving the equation

$$\rho_-(\alpha, \omega_a, \omega_{h1}, \omega_{h2}) = \rho_*(\alpha, \omega_a, \omega_{h1}, \omega_{h2}) \quad (16)$$

numerically, and two typical phase diagrams have been plotted in figs.2(a) and (b) assuming [17, 18] $\omega_{h1} = \omega_{h2} = \omega_h$.

We focus on genes of *Escherichia coli* K-12 strain MG1655 [19]. We directly simulate the system by assuming that the site dependent transition rate ω_a is proportional to the percentage availability of the corresponding aa-tRNA for that codon, in the E Coli cell [20, 21]. In figure (3), we see how the current increases as ω_h (in (a)) and α (in (b)) increases and gradually saturates; the saturation value of the current is numerically equal to the maximum current obtained in the corresponding case with PBC [13]. Simultaneously, the average density of the ribosomes decreases in (a) (and increases in (b)) as the parameter ω_h in (a) (and α in (b)) increases, and gradually saturates. These observations are consistent with the scenario of phase transition from one dynamical phase to another, as predicted by the extremal current hypothesis. Moreover, the lower flux observed for real genes, as compared to that for homogeneous mRNA, is caused by the codon specificity of the available tRNA molecules.

In this letter we have developed a “unified” theoretical model for protein synthesis by mutually interacting ribosomes following the master equation approach of non-equilibrium statistical mechanics. We have computed (i) the rate of protein synthesis in real time and (ii) density profile of the ribosomes on a given mRNA, and studied their dependences on the rates of various *mechanochemical* processes in each ribosome. We have illustrated the use of our model by applying these to two genes of *E-Coli* and making theoretical predictions in real time which, we hope, will motivate new *quantitative* measurements.

-
- [1] A.S. Spirin, FEBS Lett. **514**, 2 (2002).
 - [2] T. Hermann, Curr. Op. in str. biol. **15**, 355 (2005).
 - [3] C.T. MacDonald and J.H. Gibbs, Biopolymers **7**, 707 (1969).
 - [4] G. lakatos and T. Chou, J. Phys. A **36**, 2027 (2003).
 - [5] L.B. Shaw, R.K.P. Zia and K.H. Lee, Phys. Rev. E **68**, 021910 (2003).
 - [6] L.B. Shaw, J.P. Sethna and K.H. Lee, Phys. Rev. E **70**, 021901 (2004).
 - [7] L.B. Shaw, A.B. Kolomeisky and K.H. Lee, J. Phys. A **37**, 2105 (2004).
 - [8] T. Chou, Biophys. J., **85**, 755 (2003).
 - [9] T. Chou and G. Lakatos, Phys. Rev. Lett. **93**, 198101 (2004).
 - [10] G. Schütz, Phase Transitions and Critical Phenomena, vol. 19 (Acad. Press, 2001).
 - [11] K. Nishinari, Y. Okada, A. Schadschneider and D. Chowdhury, Phys. Rev. Lett. **95**, 118101 (2005).
 - [12] Y. Kafri and D.R. Nelson, J. Phys. Cond. Matt. **17**, S3871 (2005).
 - [13] A. Basu and D. Chowdhury, to be published.
 - [14] Y. Arava, F.E. Boas, P.O. Brown and D. Herschlag, Nucl. Acids Res. **33**, 2421 (2005).
 - [15] V.L. Mackay, X. Li, M.R. Flory, E. Turcott, G.L. Law, K.A. Serikawa, X.L. Xu, H. Lee, D.R. Goodlett, R. Aebersold, L.P. Zhao and D.R. Morris, Mol. cell. proteomics, **3**, 478 (2004).
 - [16] V. Popkov and G. Schütz, Europhys. Lett. **48**, 257 (1999).
 - [17] R.C. Thompson, D.B. Dix and J.F. Eccleston, J. Biol. Chem. **255**, 11088 (1980).
 - [18] K.M. Harrington, I.A. nazarenko, D.B. Dix, R.C. Thompson and O.C. Uhlenbeck, Biochem. **32**, 7617 (1993).
 - [19] see <http://www.genome.wisc.edu/sequencing/k12.htm>

- [20] J. Solomovici, T. Lesnik and C. Reiss, J. Theor. Biol. 198 (1990).
185, 511 (1997).
- [21] S.G.E. Andersson and C.G. Kurland, Microbiol. Rev. **54**,